

## Reduction–Oxidation Properties of Organotransition-metal Complexes. Part 21.<sup>1</sup> Synthesis and X-Ray Structural Characterisation of the Redox-related Pair of Cyclohexadienyl Complexes $[\text{Mn}(\text{CO})(\text{dppe})(\eta^5\text{-C}_6\text{H}_6\text{Ph})]$ and $[\text{Mn}(\text{CO})(\text{dppe})(\eta^5\text{-C}_6\text{H}_6\text{Ph})][\text{PF}_6]\cdot 0.5\text{CH}_2\text{Cl}_2$ \*

Neil G. Connelly, Mark J. Freeman, A. Guy Orpen, Alan R. Sheehan, and John B. Sheridan  
*Department of Inorganic Chemistry, University of Bristol, Bristol BS8 1TS*  
Dwight A. Sweigart  
*Department of Chemistry, Brown University, Providence, Rhode Island 02912, U.S.A.*

The cyclohexadienyl complexes  $[\text{Mn}(\text{CO})_{3-n}\text{L}_n(\eta^5\text{-C}_6\text{H}_6\text{Ph})]$  [**1a**,  $n = 1$ ,  $\text{L} = \text{PPh}_3$ ; **1b**,  $n = 2$ ,  $\text{L}_2 = \text{Ph}_2\text{PCH}_2\text{CH}_2\text{PPh}_2$  (dppe)], prepared by u.v. photolysis of  $[\text{Mn}(\text{CO})_3(\eta^5\text{-C}_6\text{H}_6\text{Ph})]$  and  $\text{L}$ , undergo reversible one-electron oxidation at a platinum electrode in  $\text{CH}_2\text{Cl}_2$ . The paramagnetic salt  $[\text{Mn}(\text{CO})(\text{dppe})(\eta^5\text{-C}_6\text{H}_6\text{Ph})][\text{PF}_6]$  (**2**) is isolable from the reaction between (**1b**) and  $[\text{Fe}(\eta\text{-C}_5\text{H}_5)_2][\text{PF}_6]$ . X-Ray structural studies on (**1b**) and (**2**) $\cdot 0.5\text{CH}_2\text{Cl}_2$  show the most pronounced effects of oxidation to be on the mean Mn–P distances which change from 2.221 Å in (**1b**) to 2.338 Å in (**2**). The effect on the conformation of the  $\text{Mn}(\text{CO})(\text{dppe})$  unit relative to the cyclohexadienyl moiety is small; in both complexes the CO ligand lies beneath the saturated ring carbon, giving approximate  $\text{C}_s$  symmetry to (**1b**) and (**2**). The structural consequences of one-electron oxidation on the geometry about the metal and within the ligands are discussed with regard to the nature of the highest occupied molecular orbital of (**1b**) and its depopulation in (**2**).

The cyclo-octenyl complex  $[\text{Fe}\{\text{P}(\text{OMe})_3\}_3(\text{C}_8\text{H}_{13})]^+$  is stabilised by a three-centre, two-electron interaction involving the metal atom and an *endo*-H–C bond of a  $\text{CH}_2$  group adjacent to the allyl function<sup>2</sup> [ $\text{Fe}-\text{H}$  1.874(3) Å].† This 'agostic'<sup>3</sup> interaction is partially retained in the neutral compound  $[\text{Fe}\{\text{P}(\text{OMe})_3\}_3(\text{C}_8\text{H}_{13})]$  [ $\text{Fe}-\text{H}$  2.77(2) Å],<sup>4</sup> which has a formal valence electron count of 17, and is entirely absent in the 18-electron analogue  $[\text{Co}\{\text{P}(\text{OMe})_3\}_3(\eta^3\text{-C}_8\text{H}_{13})]$ .<sup>5</sup> These observations are particularly relevant to our studies of the activation of organotransition metal complexes by one-electron transfer and prompt us to report on the oxidation of the cyclohexadienyl complexes  $[\text{Mn}(\text{CO})_{3-n}\text{L}_n(\eta^5\text{-C}_6\text{H}_6\text{Ph})]$  [**1a**,  $n = 1$ ,  $\text{L} = \text{PPh}_3$ ; **1b**,  $n = 2$ ,  $\text{L}_2 = \text{Ph}_2\text{PCH}_2\text{CH}_2\text{PPh}_2$  (dppe)]. Comparison of the crystal structures of the complexes (**1b**) and  $[\text{Mn}(\text{CO})(\text{dppe})(\eta^5\text{-C}_6\text{H}_6\text{Ph})][\text{PF}_6]$  (**2**) has allowed a detailed examination of the effects of one-electron oxidation on the ground-state geometry of (**1b**). Although the structural effects of this redox process are less dramatic than those in the  $[\text{Fe}\{\text{P}(\text{OMe})_3\}_3(\text{C}_8\text{H}_{13})]^{0,+1}$  couple, they nevertheless provide an insight into the nature of the highest occupied molecular orbital (h.o.m.o.) of (**1b**) and the general effects of oxidation on an organometallic species of this type.

### Results and Discussion

On u.v. irradiation of a mixture of  $[\text{Mn}(\text{CO})_3(\eta^5\text{-C}_6\text{H}_6\text{Ph})]$  and  $\text{PPh}_3$  or dppe in tetrahydrofuran (thf), carbon monoxide is evolved and moderate yields of crystalline  $[\text{Mn}(\text{CO})_{3-n}\text{L}_n(\eta^5\text{-C}_6\text{H}_6\text{Ph})]$  (**1a**,  $n = 1$ ,  $\text{L} = \text{PPh}_3$ ; **1b**,  $n = 2$ ,  $\text{L}_2 = \text{dppe}$ ) are

isolated. The substitution products were characterised by elemental analysis (Table 1), by their i.r. carbonyl spectra (Table 1), and by n.m.r. spectroscopy (Table 2). The <sup>1</sup>H and <sup>13</sup>C n.m.r. spectra of (**1a**) and (**1b**) are very similar to those<sup>6</sup> of  $[\text{Mn}(\text{CO})_3(\eta^5\text{-C}_6\text{H}_6\text{Ph})]$  for which the *exo* stereochemistry of the 6-phenyl substituent has been established by X-ray crystallography.<sup>7</sup> The cyclohexadienyl proton resonances are, however, shifted to higher field as the carbonyls are sequentially replaced by the phosphine ligands.

Cyclic voltammetry shows that (**1a**) and (**1b**) undergo one-electron oxidation at a platinum electrode in  $\text{CH}_2\text{Cl}_2$ , with the electron-transfer process reversible ( $i_{\text{pa}}/i_{\text{pc}} = 1.0$ ) and diffusion controlled ( $i_{\text{pa}}/v^{1/2}$  constant) for scan rates,  $v$ , from 100 to 500  $\text{mV s}^{-1}$ . For (**1b**) a second, chemically irreversible oxidation occurs with a peak potential of ca. 1.1 V.

The relatively high  $E^\circ$  value for (**1a**) (Table 1) suggests that chemical oxidation might be achieved, but with difficulty. On adding  $\text{AgBF}_4$  to the complex in  $\text{CH}_2\text{Cl}_2$ , a purple solution is formed which shows two new carbonyl bands [ $\nu(\text{CO}) = 2029$  and  $1969 \text{ cm}^{-1}$ ] at wavenumbers ca.  $80 \text{ cm}^{-1}$  higher than those of (**1a**). However, no further evidence could be gathered for the implied existence of  $[\text{Mn}(\text{CO})_2(\text{PPh}_3)(\eta^5\text{-C}_6\text{H}_6\text{Ph})]^+$ .

By contrast, the electrochemical studies (Table 1) suggested that (**1b**) would readily form the corresponding monocation with a weak one-electron oxidant. Accordingly, the reaction of  $[\text{Fe}(\eta\text{-C}_5\text{H}_5)_2][\text{PF}_6]$  with the monocarbonyl in  $\text{CH}_2\text{Cl}_2$  gave a green-yellow solution from which green crystals of  $[\text{Mn}(\text{CO})(\text{dppe})(\eta^5\text{-C}_6\text{H}_6\text{Ph})][\text{PF}_6]$  (**2**) were isolated on adding n-hexane. The cationic complex (**2**) was identified by elemental analysis, by the observation of one i.r. carbonyl absorption at  $1941 \text{ cm}^{-1}$ , ca.  $100 \text{ cm}^{-1}$  to higher energy than that of (**1b**), and by cyclic voltammetry (Table 1). The last shows that (**2**) undergoes reversible one-electron reduction, at the same potential as that of the oxidation of (**1b**), and irreversible oxidation at ca. 1.1 V (as also found for the neutral monocarbonyl).

The paramagnetism of (**2**) was confirmed by the observation of an e.s.r. spectrum in  $\text{CH}_2\text{Cl}_2$ . Although there is evidence for coupling of the free electron to both manganese and phosphorus, the spectrum is too ill defined to measure  $A_{\text{iso}}$  or  $g_{\text{av}}$  values; two very broad outer lines flank nine lines each

\* [1,2-Bis(diphenylphosphino)ethane]carbonyl(1—5-η-6-*exo*-phenyl-cyclohexadienyl)-manganese(i) and -manganese(ii) hexafluorophosphate-dichloromethane (1/0.5).

Supplementary data available (No. SUP 56182, 8 pp.): isotropic and anisotropic thermal parameters, H-atom co-ordinates. See Instructions for Authors, *J. Chem. Soc., Dalton Trans.*, 1985, Issue 1, pp. xvii—xix. Structure factors are available from the editorial office.

† Estimated standard deviations (e.s.d.s) in the least significant digit are given in parentheses here and throughout this paper.

**Table 1.** Analytical, i.r. spectral, and electrochemical data for cyclohexadienylmanganese complexes

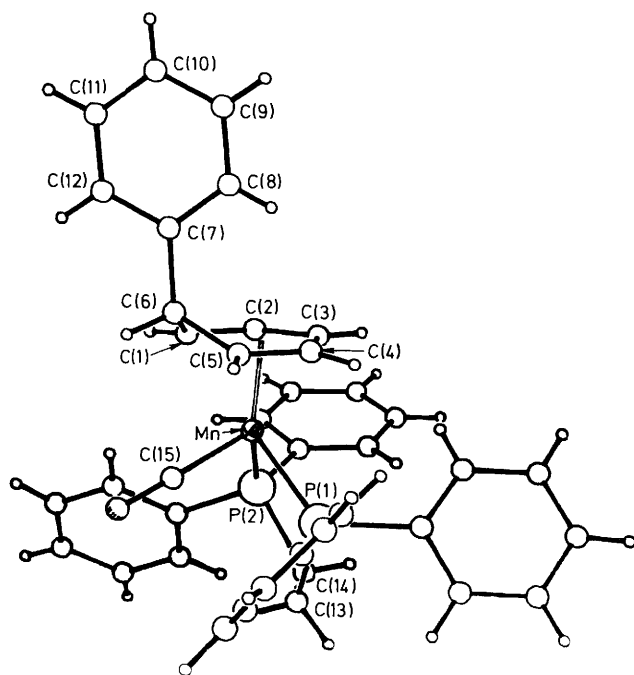
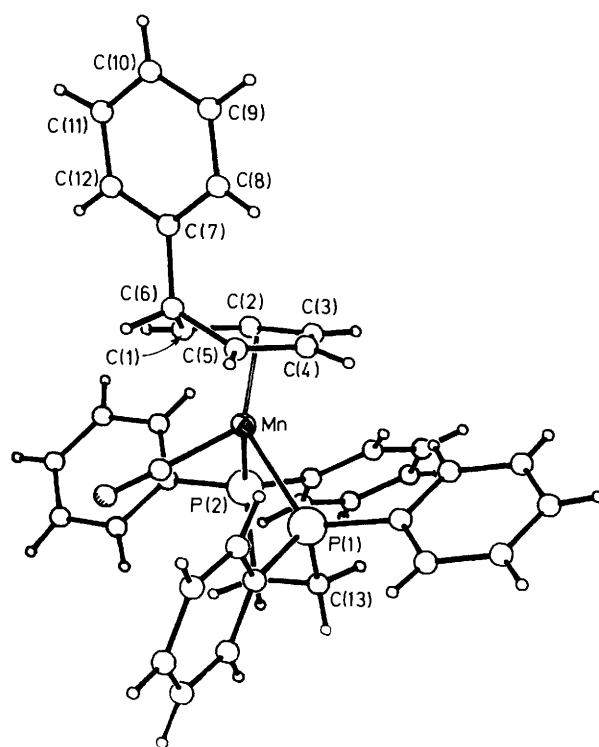
Complex	Colour	Yield (%)	$\tilde{\nu}(\text{CO})^a/\text{cm}^{-1}$	Analysis <sup>b</sup> (%)		$E^{\circ c}/\text{V}$
				C	H	
$[\text{Mn}(\text{CO})_2(\text{PPh}_3)(\eta^5\text{-C}_6\text{H}_6\text{Ph})]$	Yellow	33	1 945, 1 887 <sup>d</sup>	72.4 (72.7)	5.1 (4.9)	0.59 <sup>e</sup>
$[\text{Mn}(\text{CO})(\text{dppe})(\eta^5\text{-C}_6\text{H}_6\text{Ph})]$	Red	35	1 840	73.7 (73.6)	5.6 (5.6)	-0.06 <sup>e</sup>
$[\text{Mn}(\text{CO})(\text{dppe})(\eta^5\text{-C}_6\text{H}_6\text{Ph})][\text{PF}_6] \cdot 0.5\text{CH}_2\text{Cl}_2$	Green	82	1 941	57.4 (57.6)	4.4 (4.4)	-0.06 <sup>f</sup>

<sup>a</sup> In  $\text{CH}_2\text{Cl}_2$  unless otherwise stated. <sup>b</sup> Calculated values are given in parentheses. <sup>c</sup> Values are *versus* a standard calomel electrode, at a platinum wire, with  $0.1 \text{ mol dm}^{-3} [\text{NBu}_4][\text{PF}_6]$  as supporting electrolyte. Under these conditions  $E^{\circ}$  for the couple  $[\text{Fe}(\eta\text{-C}_5\text{H}_5)_2]^+ - [\text{Fe}(\eta\text{-C}_5\text{H}_5)_2]$  is 0.43 V. <sup>d</sup> In *n*-hexane. <sup>e</sup> One-electron oxidation. <sup>f</sup> One-electron reduction.

**Table 2.** Hydrogen-1 and <sup>13</sup>C n.m.r. spectral data<sup>a</sup> for cyclohexadienylmanganese complexes

Complex	<sup>1</sup> H (δ)	<sup>13</sup> C (p.p.m.) <sup>b</sup>
$[\text{Mn}(\text{CO})_2(\text{PPh}_3)(\eta^5\text{-C}_6\text{H}_6\text{Ph})]$	2.93 [2 H, t, $J(\text{H}^1\text{H}^2)$ 6, H <sup>1</sup> and H <sup>5</sup> ], 3.75 [1 H, t, $J(\text{H}^6\text{H}^1)$ 5, H <sup>6</sup> ], 4.58 (2 H, dd, H <sup>2</sup> and H <sup>4</sup> ), 5.61 [1 H, t, $J(\text{H}^3\text{H}^2)$ 6, H <sup>3</sup> ], 7.50 (20 H, m, Ph) <sup>c</sup>	40.56 (C <sup>6</sup> ), 55.16 (C <sup>1</sup> , C <sup>5</sup> ), 81.85 (C <sup>3</sup> ), 96.02 (C <sup>2</sup> , C <sup>4</sup> ), 126.4–138.6 (Ph), 149.22 (CO), 149.40 (CO) <sup>c</sup>
$[\text{Mn}(\text{CO})(\text{dppe})(\eta^5\text{-C}_6\text{H}_6\text{Ph})]$	2.06 (4 H, dd, CH <sub>2</sub> ), 2.64 [2 H, t br, H <sup>1</sup> and H <sup>5</sup> ], 3.43 [1 H, t br, $J(\text{H}^6\text{H}^1)$ 5.5, H <sup>6</sup> ], 4.44 (2 H, s br, H <sup>2</sup> and H <sup>4</sup> ), 5.44 (1 H, t br, H <sup>3</sup> ), 7.00 (25 H, m, Ph) <sup>d</sup>	30.72 [t, $J(^3\text{PC})$ 20.6, CH <sub>2</sub> ], 40.80 (C <sup>6</sup> ), 50.27 (C <sup>1</sup> , C <sup>5</sup> ), 77.39 (C <sup>3</sup> ), 90.95 (C <sup>2</sup> , C <sup>4</sup> ), 125.6–142.4 (Ph), 149.0 (CO) <sup>d</sup>

<sup>a</sup> Numbering as in Figure 1. <sup>b</sup> Downfield from  $\text{SiMe}_4$ . <sup>c</sup> In  $(\text{CD}_3)_2\text{CO}$ . <sup>d</sup> In  $\text{C}_6\text{D}_6$ .

**Figure 1.** Molecular geometry of (1b) showing the atomic labelling scheme adopted**Figure 2.** Molecular geometry of the cation of (2) showing the atomic labelling scheme adopted

separated by *ca.* 33 G. A further complication to the e.s.r. experiment is the slow decomposition of (2) (12 h in  $\text{CH}_2\text{Cl}_2$ ) to a second, yellow, paramagnetic species. The latter shows a six-line spectrum [ $A(^{55}\text{Mn})$  *ca.* 100 G] centred at  $g_{\text{av.}} = 2.02$  but not further characterised.

A comparison of the physical properties of (1) and (2) with those of the cyclopentadienyl complexes  $[\text{Mn}(\text{CO})_{3-n}\text{L}_n(\eta\text{-C}_5\text{R}_5)]^{z+}$  ( $n = 1$  or  $2$ ,  $\text{L} = \text{P-donor}$ ,  $\text{R} = \text{H}$  or  $\text{Me}$ ,  $z = 0$  or  $1$ )<sup>8</sup> shows many close similarities. Thus, the magnitudes of the shifts in  $\tilde{\nu}(\text{CO})$  on oxidation, the dependence of  $E^{\circ}$  on  $n$  (shifts of *ca.* 0.7 V to more negative potentials for each CO displaced), and the e.s.r. spectra of the paramagnetic cations, imply similar

electronic structures for the cyclopentadienyl and cyclohexadienyl complexes.

Although no distinction was made between ligand or metal oxidation for the cyclopentadienyl derivatives, the latter seemed more likely on the basis of e.s.r. spectroscopy. The isolation of crystals of both (1b) and (2) has allowed a comparative X-ray structural study to be made and conclusions to be drawn as to the nature of the h.o.m.o. of the neutral compound.

*Crystal Structures of*  $[\text{Mn}(\text{CO})(\text{dppe})(\eta^5\text{-C}_6\text{H}_6\text{Ph})]$  (1b) and  $[\text{Mn}(\text{CO})(\text{dppe})(\eta^5\text{-C}_6\text{H}_6\text{Ph})][\text{PF}_6]$  (2).—The crystal structures

**Table 3.** Selected bond lengths and angles for (**1b**)

## Bond lengths (Å)

Mn-P(1)	2.213(1)	Mn-P(2)	2.229(1)	C(11)-C(10)	1.386(4)	C(10)-C(9)	1.380(4)
Mn-C(5)	2.199(3)	Mn-C(4)	2.125(3)	C(9)-C(8)	1.393(3)	C(13)-C(14)	1.532(4)
Mn-C(3)	2.143(3)	Mn-C(2)	2.137(3)	C(15)-O(15)	1.176(3)	C(111)-C(112)	1.404(4)
Mn-C(1)	2.199(3)	Mn-C(15)	1.773(3)	C(111)-C(116)	1.390(3)	C(112)-C(113)	1.386(4)
P(1)-C(13)	1.859(2)	P(1)-C(111)	1.840(3)	C(113)-C(114)	1.385(4)	C(114)-C(115)	1.380(4)
P(1)-C(121)	1.856(3)	P(2)-C(14)	1.870(2)	C(115)-C(116)	1.397(4)	C(121)-C(122)	1.413(3)
P(2)-C(211)	1.848(3)	P(2)-C(221)	1.855(3)	C(121)-C(126)	1.388(3)	C(122)-C(123)	1.384(4)
C(5)-C(4)	1.395(3)	C(5)-C(6)	1.517(4)	C(123)-C(124)	1.388(3)	C(124)-C(125)	1.391(4)
C(5)-H(5)	0.948(25)	C(4)-C(3)	1.422(4)	C(125)-C(126)	1.392(4)	C(211)-C(212)	1.393(4)
C(4)-H(4)	0.984(27)	C(3)-C(2)	1.412(4)	C(211)-C(216)	1.402(4)	C(212)-C(213)	1.391(4)
C(3)-H(3)	0.903(25)	C(2)-C(1)	1.391(4)	C(213)-C(214)	1.384(5)	C(214)-C(215)	1.382(4)
C(2)-H(2)	0.921(28)	C(1)-C(6)	1.520(4)	C(215)-C(216)	1.386(4)	C(221)-C(222)	1.393(3)
C(1)-H(1)	0.884(27)	C(6)-C(7)	1.535(3)	C(221)-C(226)	1.399(3)	C(222)-C(223)	1.391(4)
C(6)-H(6)	0.972(24)	C(7)-C(12)	1.393(4)	C(223)-C(224)	1.388(4)	C(224)-C(225)	1.382(4)
C(7)-C(8)	1.382(4)	C(12)-C(11)	1.394(3)	C(225)-C(226)	1.385(4)		

## Bond angles (°)

P(1)-Mn-P(2)	84.7(1)	P(1)-Mn-C(5)	104.3(1)	C(14)-P(2)-C(211)	103.0(1)	Mn-P(2)-C(221)	119.9(1)
P(2)-Mn-C(5)	171.0(1)	P(1)-Mn-C(4)	92.5(1)	C(14)-P(2)-C(221)	102.1(1)	C(221)-P(2)-C(221)	97.8(1)
P(2)-Mn-C(4)	142.6(1)	C(5)-Mn-C(4)	37.6(1)	Mn-C(5)-C(4)	68.3(1)	Mn-C(5)-C(6)	94.0(2)
P(1)-Mn-C(3)	110.2(1)	P(2)-Mn-C(3)	107.8(1)	C(4)-C(5)-C(6)	120.9(2)	Mn-C(4)-C(5)	74.1(1)
C(5)-Mn-C(3)	68.3(1)	C(4)-Mn-C(3)	38.9(1)	Mn-C(4)-C(3)	71.2(1)	C(5)-C(4)-C(3)	119.9(2)
P(1)-Mn-C(2)	145.8(1)	P(2)-Mn-C(2)	93.0(1)	Mn-C(3)-C(4)	69.9(1)	Mn-C(3)-C(2)	70.5(1)
C(5)-Mn-C(2)	79.0(1)	C(4)-Mn-C(2)	69.0(1)	C(4)-C(3)-C(2)	116.9(2)	Mn-C(2)-C(3)	71.0(1)
C(3)-Mn-C(2)	38.5(1)	P(1)-Mn-C(1)	168.9(1)	Mn-C(2)-C(1)	73.7(1)	C(3)-C(2)-C(1)	120.6(2)
P(2)-Mn-C(1)	106.4(1)	C(5)-Mn-C(1)	64.7(1)	Mn-C(1)-C(2)	68.9(1)	Mn-C(1)-C(6)	94.0(1)
C(4)-Mn-C(1)	79.5(1)	C(3)-Mn-C(1)	68.2(1)	C(2)-C(1)-C(6)	120.2(2)	C(5)-C(6)-C(1)	101.7(2)
C(2)-Mn-C(1)	38.4(1)	P(1)-Mn-C(15)	87.7(1)	C(5)-C(6)-C(7)	117.4(2)	C(1)-C(6)-C(7)	113.7(2)
P(2)-Mn-C(15)	93.1(1)	C(5)-Mn-C(15)	88.5(1)	C(6)-C(7)-C(12)	119.9(2)	C(6)-C(7)-C(8)	122.2(2)
C(5)-Mn-C(15)	124.1(1)	C(3)-Mn-C(15)	153.3(1)	C(12)-C(7)-C(8)	117.9(2)	C(7)-C(12)-C(11)	121.3(2)
C(2)-Mn-C(15)	126.5(1)	C(1)-Mn-C(15)	90.3(1)	C(12)-C(11)-C(10)	119.9(3)	C(11)-C(10)-C(9)	119.3(2)
Mn-P(1)-C(13)	107.7(1)	Mn-P(1)-C(111)	115.0(1)	C(10)-C(9)-C(8)	120.4(3)	C(7)-C(8)-C(9)	121.2(3)
C(13)-P(1)-C(111)	106.7(1)	Mn-P(1)-C(121)	125.3(1)	H(13a)-C(13)-H(13b)	110.5(18)	H(14a)-C(14)-H(14b)	106.1(20)
C(13)-P(1)-C(121)	100.6(1)	C(111)-P(1)-C(121)	99.5(1)	Mn-C(15)-O(15)	178.1(2)		
Mn-P(2)-C(14)	110.1(1)	Mn-P(2)-C(211)	121.1(1)				

of (**1b**) and (**2**) as its hemidichloromethane solvate, (**2**)·0.5CH<sub>2</sub>Cl<sub>2</sub>, were determined by X-ray diffraction studies at *ca.* 220 K. Details of the experimental procedure and data analysis are given below in the Experimental section. Lists of selected bond lengths and interbond angles are given in Tables 3 and 4 for (**1b**) and (**2**)·0.5CH<sub>2</sub>Cl<sub>2</sub> respectively. Figures 1 and 2 show the molecular geometries of (**1b**) and the cation of (**2**) together with the atomic labelling scheme adopted.

The manganese co-ordination spheres in (**1b**) and (**2**) are the same. In each case the metal is η<sup>5</sup>-bonded to the cyclohexadienyl ring and further ligated by the two phosphorus atoms of the dppe ligand and by the carbon atom of the carbonyl group. The saturated carbon of the cyclohexadienyl ring carries the phenyl substituent in the *exo*-site as expected on spectroscopic grounds. Both (**1b**) and (**2**) show the same orientation of the Mn(CO)(dppe) unit with respect to the cyclohexadienyl moiety, each having the CO ligand lying beneath the saturated ring carbon. The C<sub>6</sub>Mn(CO)P<sub>2</sub> unit in both (**1b**) and (**2**) shows approximate (non-crystallographic) mirror symmetry, with the CO ligand, Mn, C(3), C(6), and C(7) lying on the mirror.

The reasons for the preference of ML<sub>3</sub> fragments for such a conformation in 18-electron pentadienyl, butadiene, allyl, *etc.* complexes (which tend to have one ligand L in the molecular mirror plane below the 'open' end of the acyclic polyene) have been elegantly discussed by Albright *et al.*<sup>9</sup> We shall return to the details of their studies of electronic structure later, but for the moment we note that the removal of one electron from (**1b**) does *not* cause a change in the preferred conformation in the solid state. It has been suggested<sup>10</sup> that in 16-electron species

the preferred orientation of the ML<sub>3</sub> fragment would be rotated by 180° relative to that in the 18-electron complexes.

Our main purpose in carrying out the X-ray studies described was to evaluate the structural effects of the one-electron oxidation of (**1b**). In order to assist in this, Table 5 lists relevant geometric parameters for (**1b**) and (**2**) together with those of the related manganese cyclohexadienyl complexes [Mn(CO)<sub>3</sub>(η<sup>5</sup>-C<sub>6</sub>H<sub>7</sub>)] (**3**),<sup>10</sup> [Mn(CO)<sub>3</sub>(η<sup>5</sup>-C<sub>6</sub>H<sub>6</sub>Ph)] (**4**),<sup>7</sup> and [Mn(CO)<sub>2</sub>(NO)(η<sup>5</sup>-C<sub>6</sub>H<sub>6</sub>Me)] [PF<sub>6</sub>]<sup>-</sup> (**5**).<sup>10</sup> With these data to hand it is possible to assess the effect on manganese-cyclohexadienyl bonding, of the overall charge on the complex, the nature of the substituents at manganese and at the ring, and of the formal oxidation state of the metal [*i.e.* +2 for complex (**2**) and +1 for the remaining compounds in Table 5].

All of these complexes show the approximate mirror symmetry and the usual preferred conformation of the Mn-(C<sub>6</sub>H<sub>6</sub>R)L<sub>3</sub> units observed for (**1b**) and (**2**) [for (**3**) the mirror is crystallographically imposed] with the exception that (**5**) has the NO ligand in one of the two L sites *off* the mirror and consequently shows some asymmetry in the Mn-C distances.

The effects of charge on the complex, and of the substituents on the manganese and cyclohexadienyl moiety, are not large as judged by the structures of (**1b**), (**3**), (**4**), and (**5**). For the Mn-C distances, the substitution of dppe for two carbonyl ligands has the effect of shortening Mn-C(1) [by 0.027(3) Å] and Mn-C(2) [the latter marginally by 0.007(3) Å] and lengthening Mn-C(3) slightly [by 0.015(3) Å]. A positive charge, as in (**5**) where it is allied with the presence of an NO ligand, seems to lengthen all of the manganese-ring distances uniformly, by *ca.* 0.02 Å. The

**Table 4.** Selected bond lengths and angles for (2)-0.5CH<sub>2</sub>Cl<sub>2</sub>

## Bond lengths (Å)

Mn-P(1)	2.351(2)	Mn-P(2)	2.326(2)	C(15)-O(15)	1.147(4)	C(111)-C(112)	1.388(4)
Mn-C(1)	2.171(3)	Mn-C(2)	2.146(3)	C(111)-C(116)	1.390(4)	C(112)-C(113)	1.388(4)
Mn-C(3)	2.163(3)	Mn-C(4)	2.149(3)	C(113)-C(114)	1.388(4)	C(114)-C(115)	1.366(5)
Mn-C(5)	2.176(3)	Mn-C(15)	1.803(3)	C(115)-C(115)	1.389(4)	C(121)-C(122)	1.399(4)
P(1)-C(13)	1.826(3)	P(1)-C(111)	1.822(3)	C(121)-C(126)	1.389(4)	C(122)-C(123)	1.376(5)
P(1)-C(121)	1.819(3)	P(2)-C(14)	1.832(3)	C(123)-C(124)	1.383(5)	C(124)-C(125)	1.366(6)
P(2)-C(211)	1.825(3)	P(2)-C(221)	1.817(3)	C(125)-C(126)	1.392(5)	C(211)-C(212)	1.390(4)
C(1)-H(1)	0.930(31)	C(1)-C(2)	1.393(4)	C(211)-C(216)	1.383(4)	C(212)-C(213)	1.385(4)
C(1)-C(6)	1.524(4)	C(2)-H(2)	0.989(33)	C(213)-C(214)	1.381(4)	C(214)-C(215)	1.378(4)
C(2)-C(3)	1.415(4)	C(3)-H(3)	0.909(31)	C(215)-C(216)	1.385(4)	C(221)-C(222)	1.384(5)
C(3)-C(4)	1.402(4)	C(4)-H(4)	0.925(25)	C(221)-C(226)	1.383(4)	C(222)-C(223)	1.389(5)
C(4)-C(5)	1.397(4)	C(5)-H(5)	0.964(27)	C(223)-C(224)	1.364(6)	C(224)-C(225)	1.369(5)
C(5)-C(6)	1.514(4)	C(6)-H(6)	0.977(29)	C(225)-C(226)	1.395(5)	P(3)-F(1)	1.593(2)
C(6)-C(7)	1.524(4)	C(7)-C(8)	1.390(4)	P(3)-F(2)	1.578(3)	P(3)-F(3)	1.592(2)
C(7)-C(12)	1.395(4)	C(8)-C(9)	1.387(4)	P(3)-F(4)	1.578(3)	P(3)-F(5)	1.599(2)
C(9)-C(10)	1.382(5)	C(10)-C(11)	1.387(4)	P(3)-F(6)	1.576(3)	Cl(1)-C	1.660(11)
C(11)-C(12)	1.387(4)	C(13)-C(14)	1.522(4)	C-Cl(1')	1.594(12)		

## Bond angles (°)

P(1)-Mn-P(2)	83.6(1)	P(1)-Mn-C(1)	170.0(1)	Mn-C(2)-C(3)	71.5(2)	C(1)-C(2)-C(3)	120.2(3)
P(2)-Mn-C(1)	106.0(1)	P(1)-Mn-C(2)	146.7(1)	Mn-C(3)-C(2)	70.2(2)	Mn-C(3)-C(4)	70.5(2)
P(2)-Mn-C(2)	93.1(1)	C(1)-Mn-C(2)	37.6(1)	C(2)-C(3)-C(4)	118.0(2)	Mn-C(4)-C(3)	71.6(2)
P(1)-Mn-C(3)	111.7(1)	P(2)-Mn-C(3)	108.2(1)	Mn-C(4)-C(5)	72.2(2)	C(3)-C(4)-C(5)	120.5(2)
C(1)-Mn-C(3)	68.4(1)	C(2)-Mn-C(3)	38.4(1)	Mn-C(5)-C(4)	70.1(2)	Mn-C(5)-C(6)	91.8(2)
P(1)-Mn-C(4)	94.1(1)	P(2)-Mn-C(4)	141.9(1)	C(4)-C(5)-C(6)	119.4(2)	C(1)-C(6)-C(5)	103.5(2)
C(1)-Mn-C(4)	79.9(1)	C(2)-Mn-C(4)	68.4(1)	C(1)-C(6)-C(7)	114.0(2)	C(5)-C(6)-C(7)	116.1(2)
C(3)-Mn-C(4)	37.9(1)	P(1)-Mn-C(5)	103.8(1)	C(6)-C(7)-C(8)	122.3(2)	C(6)-C(7)-C(12)	119.3(2)
P(2)-Mn-C(5)	172.4(1)	C(1)-Mn-C(5)	66.6(1)	C(8)-C(7)-C(12)	118.2(3)	C(7)-C(8)-C(9)	121.1(3)
C(2)-Mn-C(5)	80.0(1)	C(3)-Mn-C(5)	68.1(1)	C(8)-C(9)-C(10)	120.0(3)	C(9)-C(10)-C(11)	119.7(3)
C(4)-Mn-C(5)	37.7(1)	P(1)-Mn-C(15)	87.6(1)	C(10)-C(11)-C(12)	120.0(3)	C(7)-C(12)-C(11)	120.9(3)
P(2)-Mn-C(15)	90.2(1)	C(1)-Mn-C(15)	89.7(1)	H(13a)-C(13)-H(13b)	110.0(27)	H(14a)-C(14)-H(14b)	106.0(25)
C(2)-Mn-C(15)	125.6(1)	C(3)-Mn-C(15)	154.3(1)	Mn-C(15)-O(15)	177.3(3)	F(1)-P(3)-F(2)	179.3(1)
C(4)-Mn-C(15)	127.8(1)	C(5)-Mn-C(15)	91.4(1)	F(1)-P(3)-F(3)	89.8(1)	F(2)-P(3)-F(3)	90.6(1)
Mn-P(1)-C(13)	106.9(1)	Mn-P(1)-C(111)	122.2(1)	F(1)-P(3)-F(4)	89.1(1)	F(2)-P(3)-F(4)	90.4(1)
C(13)-P(1)-C(111)	104.3(1)	Mn-P(1)-C(121)	112.3(1)	F(3)-P(3)-F(4)	90.1(1)	F(1)-P(3)-F(5)	88.7(1)
C(13)-P(1)-C(121)	105.8(1)	C(111)-P(1)-C(121)	104.0(1)	F(2)-P(3)-F(5)	90.9(1)	F(3)-P(3)-F(5)	178.3(1)
Mn-P(2)-C(14)	105.7(1)	Mn-P(2)-C(211)	123.1(1)	F(4)-P(3)-F(5)	90.6(1)	F(1)-P(3)-F(6)	91.2(1)
C(14)-P(2)-C(21)	101.5(1)	Mn-P(2)-C(221)	113.3(1)	F(2)-P(3)-F(6)	89.3(2)	F(3)-P(3)-F(6)	90.1(1)
C(14)-P(2)-C(221)	107.5(1)	C(221)-P(2)-C(221)	104.3(1)	F(4)-P(3)-F(6)	179.6(2)	F(5)-P(3)-F(6)	89.2(1)
Mn-C(1)-C(2)	70.2(2)	Mn-C(1)-C(6)	91.7(2)	Cl(1)-C-Cl(1')	127.6(6)		
C(2)-C(1)-C(6)	119.3(2)	Mn-C(2)-C(1)	72.2(2)				

corresponding effects on the intra-ring C-C distances are below the level of significance of the results, as are the effects of the nature of the *exo*-substituent, as in (3) and (4). The Mn-CO and C-O distances follow the expected trends being respectively longer and shorter as the manganese environment is more electron poor [*i.e.* in electron-richness (1b) > (3) ≈ (4) > (5)].

As shown in Table 5 the largest effect of oxidising (1b) on bond length is on the Mn-P distances, causing an increase of 0.117(2) Å. This implies that the orbital half depopulated on going from (1b) to (2) has an element of Mn-P bonding character. The effect on the manganese-cyclohexadienyl distances is small but not isotropic. Thus Mn-C(1) shortens [by 0.025(3) Å] and Mn-C(2) and Mn-C(3) lengthen [by 0.017(3) and 0.021(3) Å respectively]. Associated with these changes in Mn-C distances are angular changes about the manganese which imply that the cyclohexadienyl ring slips in the C(1) → C(2) direction. Thus the Mn-ch-C(3)\* and ch-Mn-CO angles increase on oxidation, while the mean ch-Mn-P angles stay relatively unchanged. The Mn-C-O system shows changes consistent with the increase in positive charge on going from (1b) to (2). Finally, the P-C distances show significant decreases on oxidation [by *ca.* 0.030(3) Å].

There is a variety of mechanisms by which we might expect one-electron oxidation to affect the ground-state molecular structure of an organotransition-metal complex. If there is no

massive structural rearrangement, and hence no great reorganisation of molecular orbitals (as here), halving the occupancy of the h.o.m.o. on oxidation should show structural effects indicative of the nature of the orbital. That is, bond lengths should vary according to the nature of atomic overlaps, bonding or antibonding. In addition, conformational preferences which arise out of a balance between the requirements of the h.o.m.o. (*e.g.* for optimum spatial overlap) and those of lower (filled) orbitals will relax after oxidation to a (slightly) different equilibrium position which will more nearly suit the requirements of the lower orbitals. There will be further 'charge effects' dependent on the primary location of the h.o.m.o. (*i.e.* whether metal or ligand based). Thus, if the h.o.m.o. is metal based, the metal atomic orbitals will be contracted spatially and lowered in energy as a consequence of reduced nuclear shielding. The structural consequences of this charge effect might be expected to be more widespread (although not necessarily large) than those above, affecting all orbitals with a metal contribution.

To assess these possibilities in the case of (1b) and (2) we have used the Extended Hückel Molecular Orbital (EHMO)

\* The centroid of the five contact carbons of the cyclohexadienyl moiety is denoted by ch.

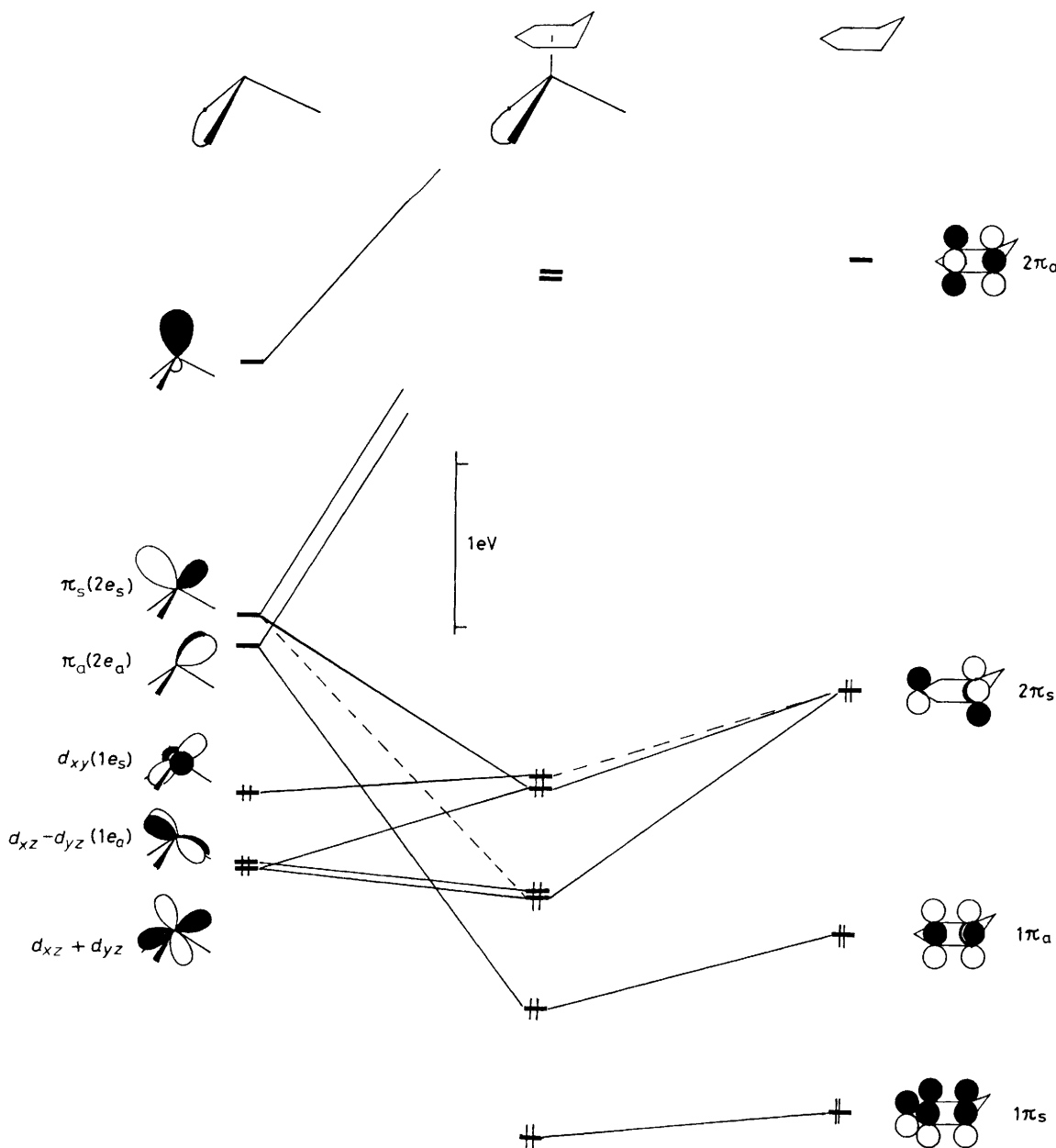


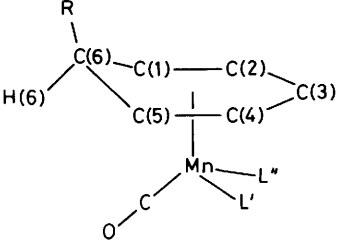
**Figure 3.** Interaction diagram for  $[\text{Mn}(\text{CO})(\text{H}_2\text{PCH}_2\text{CH}_2\text{PH}_2)]^+$  and  $[\eta^5\text{-C}_6\text{H}_7]^-$  fragments illustrating the major components of the frontier molecular orbitals; metal fragment labels given in parentheses and all the anion fragment labels are those used in ref. 9 ( $\text{eV} \approx 1.60 \times 10^{-19} \text{ J}$ )

theory<sup>11</sup> to establish the nature of the h.o.m.o. of a model for **(1b)**, namely  $[\text{Mn}(\text{CO})(\text{H}_2\text{PCH}_2\text{CH}_2\text{PH}_2)(\eta^5\text{-C}_6\text{H}_7)]$ . These calculations show some differences in detail from those of ref. 9 on  $[\text{Fe}(\text{CO})_3(\eta^5\text{-C}_6\text{H}_7)]^+$  without in any way contradicting those authors' conclusions. The results are displayed schematically in Figure 3. The effect on the frontier orbitals of the  $\text{ML}_3$  fragment of substituting two CO ligands by dppe is to lift the degeneracy of the  $1e$  and  $2e^9$  valence orbitals. In particular the  $d_{xy}$  ( $1e_s$  in the notation of ref. 11) becomes the h.o.m.o. of the fragment since it alone of the Mn ' $t_2$ ' set is not stabilised by interaction with the CO  $\pi^*$  orbital. Albright *et al.*<sup>9</sup> concluded that the conformational preference shown by acyclic  $\text{ML}_3$ -(polyene) complexes arises from an unfavourable four-electron interaction between  $1e_s$  and  $2\pi_s$  in the 'wrong' ( $180^\circ$  rotated) conformer and optimum  $\langle 2e_s | 2\pi_s \rangle$  overlap in the 'right'

conformer. These factors are still at work in **(1b)** and **(2)**, and hence the observed conformations.

Substitution of two carbonyl ligands by dppe localises ' $1e_s$ ' as  $d_{xy}$  (see Figure 3) as well as raising its energy and hence favours the conformation which minimises this orbital's overlap with the filled ( $1\pi_s, 1\pi_a, 2\pi_s$ ) orbitals of the cyclohexadienyl ligand, *i.e.* that seen for **(1b)** and **(2)**. For the model  $[\text{Fe}(\text{CO})_3(\eta^3\text{-C}_6\text{H}_7)]^+$  the molecular h.o.m.o. is the  $2e_s, 2\pi_s$  bonding combination.<sup>9</sup> In our model for **(1b)** the h.o.m.o. is primarily composed of Mn  $d_{xy}$  ( $1e_s$  in ref. 9), slightly destabilised relative to its energy in  $\text{Mn}(\text{CO})(\text{H}_2\text{PCH}_2\text{CH}_2\text{PH}_2)$  due to mixing with ' $2e_s$ ' and  $2\pi_s$ .

This EHMO study therefore implies that the oxidation of **(1b)** is metal based, and the orbital ( $d_{xy}$ ) depopulated is mildly Mn-C<sub>6</sub>H<sub>6</sub>R antibonding, particularly with respect to C(1) and C(5), as indeed reflected in bond length changes. Clearly the  $d_{xy}$

**Table 5.** Geometrical parameters for cyclohexadienylmanganese complexes


Complex	(1b)	(2)	(3)	(4)	(5)
R	Ph	Ph	H	Ph	Me
L', L''	dppe	dppe	(CO) <sub>2</sub>	(CO) <sub>2</sub>	(CO)(NO)
Charge	0	+1	0	0	+1

Distances (Å) (averaged over <i>m</i> symmetry) <sup>a</sup>					
Mn–C(1)	2.199(3)	2.174(3)	2.219(7)	2.226(2)	2.246(4)
Mn–C(2)	2.131(3)	2.148(3)	2.152(8)	2.138(2)	2.160(4)
Mn–C(3)	2.142(3)	2.163(3)	2.141(9)	2.127(1)	2.150(4)
Mn–CO	1.773(3)	1.803(3)	1.789(9)	1.803(3)	1.871(3)
Mn–P	2.221(1)	2.338(2)	—	—	—
Mn...H(6)	3.14	3.06	3.25	3.12	3.14
C(1)–C(2)	1.392(4)	1.395(4)	1.388(11)	1.391(2)	1.397(4)
C(2)–C(3)	1.417(4)	1.409(4)	1.415(12)	1.416(2)	1.420(4)
C(1)–C(6)	1.519(4)	1.519(4)	1.511(13)	1.517(2)	1.511(4)
C–O	1.176(3)	1.143(4)	1.158(12)	1.149(2)	1.133(3)
P–C(aryl) (av.)	1.850(3)	1.821(3)	—	—	—
P–C(alkyl) (av.)	1.865(3)	1.829(3)	—	—	—

Angles (°) <sup>b</sup>					
L'–Mn–L''	83.6(1)	84.7(1)	89.4(4)	88.23(7)	93.9(1)
L–Mn–CO (av.)	88.9(1)	90.4(1)	94.5(4)	95.19(7)	95.3(1)
ch–Mn–L (av.)	129.0(1)	129.5(1)	125.0(4)	—	124.3(1)
ch–Mn–CO	121.1(1)	122.9(1)	120.5(4)	—	115.8(1)
Mn–ch–C(3)	96.8(1)	98.8(1)	96.5(4)	—	95.0(1)

Interplanar angle					
C(1), C(6), C(5)/C(1), C(2), C(3), C(4), C(5)	39.7	39.2	42.8	36.8	39.6

<sup>a</sup> The averaging of Mn–C distances is not as satisfactory for (5) as for the other complexes since the orientation of the Mn(CO)<sub>2</sub>NO unit violates the 'mirror symmetry'. <sup>b</sup> Centroid of the five contact carbons of the cyclohexadienyl ring is denoted by ch.

orbital is that member of the 't<sub>2g</sub>' set most involved in π-bonding to the dppe ligand, although in the model complex as parameterised this is not a major interaction. The depopulation of this orbital therefore leads directly to diminution of what Mn–P π-bonding there is, and hence the unexpectedly large change in Mn–P distance. The magnitude of this change may reflect the softness of Mn–P bond lengths, as also indicated by the variations in Mn–P lengths within (1b) and within (2), see Tables 3 and 4. The change in P–C distances is consistent with depletion of Mn–P π-bonding since the π-acceptor orbital on phosphorus will have a component of P–C σ\* character. Others have noted lengthening of metal–phosphine distances on oxidation<sup>12</sup> although less marked than here. By way of comparison the Mn–P distances in (1b) are similar to those in other Mn<sup>I</sup> complexes, e.g. av. Mn–P in [Mn(CO)(PPh<sub>3</sub>)<sub>2</sub>(η<sup>5</sup>-C<sub>5</sub>H<sub>5</sub>)] is 2.237(3) Å [Mn–C(O) 1.748(9) Å].<sup>13</sup> The Mn<sup>II</sup>–P distances in (2) are slightly longer than those in the low-spin Mn<sup>II</sup> complex [Mn{o-(CH<sub>2</sub>)<sub>2</sub>C<sub>6</sub>H<sub>4</sub>}(Me<sub>2</sub>PCH<sub>2</sub>CH<sub>2</sub>PM<sub>2</sub>)<sub>2</sub>] [av. Mn–P 2.230(3) and 2.298(3) Å]<sup>14</sup> but much shorter than those in high-spin Mn<sup>II</sup> complexes, e.g. [Mn(CH<sub>2</sub>CMe<sub>2</sub>Ph)<sub>2</sub>(PMe<sub>2</sub>)<sub>2</sub>] [av. Mn–P 2.633(4) Å].<sup>14</sup>

The cyclohexadienyl group hydrogens H(1)–H(5) show considerable distortions from the plane of the five contact carbons in both (1b) and (2). Averaged over the molecular symmetry the distortions are +0.064, +0.117, and –0.018 Å for (1b) compared with +0.108, +0.155, and –0.029 Å for (2) for H(1), H(2), and H(3) respectively (e.s.d.s in these are ca. 0.03 Å). The manganese atoms lie +1.668 and +1.657 Å from these planes, and the r.m.s. deviation of the carbon atoms from the planes is 0.012 and 0.006 Å for (1b) and (2) respectively.

As noted above, the other changes are minor and in particular no strong interaction is induced between Mn and the *endo*-hydrogen, H(6), on oxidation (in contrast to the 17-electron system [Fe{P(OMe)<sub>3</sub>}<sub>3</sub>(C<sub>8</sub>H<sub>13</sub>)]<sup>4</sup>). Presumably this reflects the greater rigidity of the η<sup>5</sup>-cyclohexadienyl moiety as compared with the η<sup>3</sup>-cyclo-octenyl ligand.

### Experimental

The preparation, purification, and reactions of the complexes described were carried out under an atmosphere of dry nitrogen. The complexes [Mn(CO)<sub>3</sub>(η<sup>5</sup>-C<sub>6</sub>H<sub>6</sub>Ph)]<sup>6</sup> and [Fe(η<sup>5</sup>-C<sub>5</sub>H<sub>5</sub>)<sub>2</sub>][PF<sub>6</sub>]<sup>15</sup> were prepared by published methods. Cyclic voltammetry was carried out as previously described.<sup>16</sup> I.r. spectra were recorded on a Nicolet MX-1 Fourier-transform instrument. Proton and <sup>13</sup>C n.m.r. spectra were measured on a JEOL FX90Q spectrometer (at 90 and 22.50 MHz respectively) and calibrated against SiMe<sub>4</sub> as internal reference. X-Band e.s.r. spectra were recorded on a Varian Associates 4502/15 instrument and were calibrated against a solid sample of the diphenylpicrylhydrazyl radical. Microanalyses were by the staff of the Microanalytical Service of the School of Chemistry, University of Bristol.

[1,2-Bis(diphenylphosphino)ethane]carbonyl(1–5-η-6-exo-phenylcyclohexadienyl)manganese, [Mn(CO)(dppe)(η<sup>5</sup>-C<sub>6</sub>H<sub>6</sub>Ph)].—A stirred, cooled (15 °C) solution of [Mn(CO)<sub>3</sub>(η<sup>5</sup>-C<sub>6</sub>H<sub>6</sub>Ph)] (0.51 g, 1.73 mmol) and dppe (0.69 g, 1.73 mmol) in thf (200 cm<sup>3</sup>) was irradiated (u.v. light) for 7 h and purged with N<sub>2</sub> gas. The resulting bright orange solution was filtered and evaporated to dryness *in vacuo*. The red-orange residue was dissolved in toluene (25 cm<sup>3</sup>) and chromatographed on a n-hexane–alumina column (3 cm × 20 cm). Elution with toluene–n-hexane (3:2) gave an orange solution which was evaporated to low volume and cooled (0 °C) overnight to give red crystals of the product, yield 0.39 g (35%).

The air-stable solid is soluble in toluene, moderately soluble in CH<sub>2</sub>Cl<sub>2</sub>, slightly soluble in n-hexane, and insoluble in acetone. Orange solutions of the complex are moderately stable in air.

The complex [Mn(CO)<sub>2</sub>(PPh<sub>3</sub>)(η<sup>5</sup>-C<sub>6</sub>H<sub>6</sub>Ph)] was prepared by a similar method. After irradiation, and evaporation to dryness, the residue was extracted with CH<sub>2</sub>Cl<sub>2</sub>. Elution from the n-hexane–alumina column using n-hexane–diethyl ether (9:1), evaporation to dryness, dissolution in CH<sub>2</sub>Cl<sub>2</sub>, addition of n-hexane, and slow evaporation *in vacuo* gave the product as yellow crystals (33%).

The product is soluble in most common organic solvents to give yellow solutions which are slowly decomposed in air.

[1,2-Bis(diphenylphosphino)ethane]carbonyl(1–5-η-6-exo-phenylcyclohexadienyl)manganese Hexafluorophosphate-dichloromethane (1/0.5), [Mn(CO)(dppe)(η<sup>5</sup>-C<sub>6</sub>H<sub>6</sub>Ph)][PF<sub>6</sub>].0.5CH<sub>2</sub>Cl<sub>2</sub>.—To a stirred solution of [Mn(CO)(dppe)(η<sup>5</sup>-C<sub>6</sub>H<sub>6</sub>Ph)] (0.20 g, 0.31 mmol) in CH<sub>2</sub>Cl<sub>2</sub> (70 cm<sup>3</sup>) was added [Fe(η<sup>5</sup>-C<sub>5</sub>H<sub>5</sub>)<sub>2</sub>][PF<sub>6</sub>] (0.10 g, 0.29 mmol). Addition of n-hexane (150 cm<sup>3</sup>) to the resulting green solution afforded a green precipitate which was redissolved in CH<sub>2</sub>Cl<sub>2</sub> and filtered. On

**Table 6.** Atomic co-ordinates ( $\times 10^4$ ) for **(1b)**

Atom	x	y	z	Atom	x	y	z
Mn	7 725(1)	7 812(1)	8 431(1)	C(114)	8 687(2)	4 842(2)	6 260(1)
P(1)	7 405(1)	7 970(1)	7 200(1)	C(115)	7 821(2)	4 725(2)	6 247(2)
P(2)	6 389(1)	8 624(1)	8 230(1)	C(116)	7 405(2)	5 672(2)	6 497(1)
C(5)	9 068(1)	7 043(2)	8 818(1)	C(121)	7 663(1)	9 302(2)	6 702(1)
C(4)	9 074(1)	8 271(2)	8 632(1)	C(122)	7 417(2)	9 288(2)	5 911(1)
C(3)	8 690(2)	9 149(2)	8 989(1)	C(123)	7 612(2)	10 262(2)	5 525(1)
C(2)	8 268(2)	8 703(2)	9 490(1)	C(124)	8 053(2)	11 269(2)	5 916(1)
C(1)	8 270(2)	7 465(2)	9 644(1)	C(125)	8 294(2)	11 301(2)	6 694(1)
C(6)	9 012(2)	6 657(2)	9 574(1)	C(126)	8 095(2)	10 324(2)	7 082(1)
C(7)	9 862(2)	6 731(2)	10 252(1)	C(211)	6 256(1)	10 118(2)	8 632(1)
C(12)	9 923(2)	6 094(2)	10 906(1)	C(212)	6 451(2)	11 195(2)	8 329(1)
C(11)	10 675(2)	6 171(3)	11 538(1)	C(213)	6 375(2)	12 319(2)	8 644(2)
C(10)	11 391(2)	6 864(3)	11 515(1)	C(214)	6 108(2)	12 381(2)	9 272(2)
C(9)	11 336(2)	7 505(3)	10 871(2)	C(215)	5 930(2)	11 322(3)	9 593(2)
C(8)	10 576(2)	7 438(2)	10 246(1)	C(216)	6 004(2)	10 204(2)	9 277(1)
C(13)	6 182(1)	7 909(2)	6 772(1)	C(221)	5 539(2)	7 780(2)	8 510(1)
C(14)	5 824(1)	8 851(2)	7 201(1)	C(222)	5 783(2)	6 800(2)	9 003(1)
C(15)	7 304(2)	6 307(2)	8 281(1)	C(223)	5 151(2)	6 198(2)	9 237(2)
O(15)	7 049(1)	5 296(2)	8 193(1)	C(224)	4 271(2)	6 559(3)	8 978(2)
C(111)	7 856(1)	6 748(2)	6 761(1)	C(225)	4 029(2)	7 537(3)	8 494(2)
C(112)	8 732(2)	6 855(2)	6 763(1)	C(226)	4 653(2)	8 149(2)	8 262(1)
C(113)	9 144(2)	5 912(2)	6 516(1)				

**Table 7.** Atomic co-ordinates ( $\times 10^4$ ) for **(2)** $\cdot 0.5\text{CH}_2\text{Cl}_2$ 

Atom	x	y	z	Atom	x	y	z
Mn	2 004(1)	141(1)	3 166(1)	C(122)	4 013(2)	-1 357(2)	2 243(2)
P(1)	3 703(1)	322(1)	2 683(1)	C(123)	4 131(3)	-2 000(2)	1 777(2)
P(2)	1 549(1)	1 467(1)	2 650(1)	C(124)	4 123(3)	-1 790(3)	1 105(2)
C(1)	529(2)	-261(2)	3 638(1)	C(125)	3 993(3)	-946(3)	899(2)
C(2)	1 064(2)	418(2)	4 002(1)	C(126)	3 889(3)	-284(2)	1 365(2)
C(3)	2 212(2)	348(2)	4 240(1)	C(211)	1 817(2)	2 513(2)	3 066(1)
C(4)	2 788(2)	-407(2)	4 082(1)	C(212)	2 577(2)	2 574(2)	3 634(1)
C(5)	2 230(2)	-1 078(2)	3 716(1)	C(213)	2 864(3)	3 376(2)	3 916(2)
C(6)	977(2)	-1 184(2)	3 737(1)	C(214)	2 388(3)	4 124(2)	3 632(2)
C(7)	605(2)	-1 639(2)	4 356(1)	C(215)	1 628(3)	4 072(2)	3 071(2)
C(8)	1 367(2)	-1 965(2)	4 862(2)	C(216)	1 345(3)	3 269(2)	2 790(2)
C(9)	1 008(3)	-2 426(2)	5 397(2)	C(221)	95(2)	1 534(2)	2 299(1)
C(10)	-123(3)	-2 580(2)	5 429(2)	C(222)	-720(3)	1 718(2)	2 724(2)
C(11)	-896(2)	-2 262(2)	4 927(2)	C(223)	-1 842(3)	1 742(3)	2 475(2)
C(12)	-534(2)	-1 794(2)	4 397(2)	C(224)	-2 158(3)	1 586(2)	1 813(2)
C(13)	3 623(2)	1 369(2)	2 251(1)	C(225)	-1 361(3)	1 406(2)	1 386(2)
C(14)	2 428(3)	1 548(2)	1 951(1)	C(226)	-229(3)	1 373(2)	1 628(2)
C(15)	1 480(2)	-426(2)	2 411(1)	P(3)	4 629(1)	2 711(1)	684(1)
O(15)	1 128(2)	-810(2)	1 974(1)	F(1)	5 831(2)	2 600(2)	416(1)
C(111)	5 054(2)	345(2)	3 186(1)	F(2)	3 444(2)	2 829(2)	956(1)
C(112)	5 139(2)	780(2)	3 797(1)	F(3)	4 105(2)	2 931(1)	-59(1)
C(113)	6 154(2)	808(2)	4 194(1)	F(4)	4 893(2)	3 706(1)	812(1)
C(114)	7 090(2)	396(2)	3 984(2)	F(5)	5 182(2)	2 475(2)	1 420(1)
C(115)	7 004(2)	-38(2)	3 386(2)	F(6)	4 360(2)	1 717(1)	560(1)
C(116)	5 998(2)	-62(2)	2 979(2)	Cl(1)	1 184(2)	111(2)	233(1)
C(121)	3 891(2)	-488(2)	2 041(1)	C	34(10)	287(6)	-281(5)

addition of n-hexane, and slow evaporation *in vacuo*, the product was precipitated as a green solid, yield 0.2 g (82%).

The complex is soluble in polar solvents such as thf and  $\text{CH}_2\text{Cl}_2$ . The pale green solutions are slowly decolourised in light.

**Structure Determinations.**—**Crystal data for (1b).**  $\text{C}_{39}\text{H}_{35}\text{MnOP}_2$ ,  $M = 635.9$ , monoclinic, space group  $P2_1/c$  (no. 14),  $a = 15.971(8)$ ,  $b = 10.988(5)$ ,  $c = 18.831(13)$  Å,  $\beta = 108.89(5)$ ,  $U = 3 126(3)$  Å<sup>3</sup>,  $Z = 4$ ,  $D_c = 1.35$  g cm<sup>-3</sup>,  $F(000) = 1 328$  electrons; graphite-monochromated X-radiation,  $\lambda = 0.710 69$  Å,  $\mu(\text{Mo-K}\alpha) = 5.36$  cm<sup>-1</sup>,  $T = 220$  K. Crystal faces, distance from origin (mm): (1 0 0) 0.25; ( $\bar{1}$  0 0) 0.25; (1  $\bar{1}$  0) 0.30; (0 0  $\bar{1}$ ) 0.25; ( $\bar{1}$   $\bar{1}$  0) 0.15; ( $\bar{1}$  1 0) 0.15; ( $\bar{1}$  1 0) 0.15; ( $\bar{1}$  1 0) 0.15; ( $\bar{1}$  1 1) 0.25.

0.30; (1 1 0) 0.35; ( $\bar{1}$   $\bar{1}$  0) 0.35; (0 0 1) 0.20; (0 0  $\bar{1}$ ) 0.20; (1 0  $\bar{2}$ ) 0.10; ( $\bar{1}$  0 2) 0.10.

**Crystal data for (2)** $\cdot 0.5\text{CH}_2\text{Cl}_2$ .  $\text{C}_{39}\text{H}_{35}\text{F}_6\text{MnOP}_3 \cdot 0.5\text{CH}_2\text{Cl}_2$ ,  $M = 823.3$ , monoclinic, space group  $P2_1/c$  (no. 14),  $a = 11.917(7)$ ,  $b = 15.369(10)$ ,  $c = 20.010(9)$  Å,  $\beta = 95.49(4)^\circ$ ,  $U = 3 666(3)$  Å<sup>3</sup>,  $Z = 4$ ,  $D_c = 1.49$  g cm<sup>-3</sup>,  $F(000) = 1 700$  electrons, graphite-monochromated Mo-K $\alpha$  X-radiation,  $\lambda = 0.710 69$  Å,  $\mu(\text{Mo-K}\alpha) = 6.08$  cm<sup>-1</sup>,  $T = 220$  K. Crystal faces, distance from origin (mm): (1 0 0) 0.25; ( $\bar{1}$  0 0) 0.25; (0 0 1) 0.30; (0 0  $\bar{1}$ ) 0.30; (1  $\bar{1}$  0) 0.15; ( $\bar{1}$  1 0) 0.15; (1 1 0) 0.15; ( $\bar{1}$  1 0) 0.15; ( $\bar{1}$  1 1) 0.25.

Crystals of **(1b)** were obtained as deep red multifaceted prisms from toluene-n-hexane solution at 0 °C. A single crystal

of approximate dimensions  $0.2 \times 0.5 \times 0.7$  mm was mounted in a thin-walled glass capillary under  $N_2$  for data collection. A unique quadrant of reciprocal space was scanned in the range  $4 < 2\theta < 50^\circ$  at 220 K using a Nicolet P3m diffractometer. *Integrated intensities* were obtained by the  $\theta-2\theta$  technique, with scan widths  $(2.4 + \Delta_{\alpha, \alpha_2})^\circ$  and scan speeds varying between 2.0 and  $29.3^\circ \text{ min}^{-1}$  based on a 2 s prescan count. For reflections with  $40 < 2\theta < 50^\circ$  only those with prescan count  $> 25$  were recorded. Of the 4 803 independent measured intensities those 4 406 with  $I \geq 1.5\sigma(I)$  were retained for use in structure solution and refinement. Two check reflections  $(-3, 7, 1)$  and  $(-8, -2, 4)$ , remeasured after every 50 reflections, showed no significant loss in intensity during the course of data collection. Absorption corrections were applied by a Gaussian quadrature technique yielding maximum and minimum transmission coefficients of 0.898 and 0.769 respectively. Data collection and reduction for  $(2) \cdot 0.5\text{CH}_2\text{Cl}_2$  proceeded as for **(1b)** with the exceptions noted below. Crystals of  $(2) \cdot 0.5\text{CH}_2\text{Cl}_2$  were grown by diffusion of n-hexane into a dichloromethane solution of **(2)**. A crystal of approximate dimensions  $0.3 \times 0.1 \times 0.6$  mm was used. Maximum  $2\theta$  was  $55^\circ$ . Check reflections  $(1, -8, 0)$ ,  $(10, 4, 2)$ , and  $(9, 3, 3)$  showed a monotonic decrease of ca. 3% during data collection; a corresponding decay correction was applied. Transmission coefficients varied between 0.855 and 0.746.

The structures were solved by the conventional heavy-atom method (Patterson, difference-Fourier), all atoms, including hydrogens, being directly located in electron density maps. For  $(2) \cdot 0.5\text{CH}_2\text{Cl}_2$  the solvent of crystallisation lies disordered about a crystallographic inversion centre. All atoms were refined without positional constraints, and all non-hydrogen atoms were assigned anisotropic vibrational parameters. Refinement was carried out by the blocked-cascade least-squares technique with individual weights  $w = [\sigma^2(F_o) + g F_o^2]^{-1}$  [ $\sigma^2(F_o)$  based on counting statistics and  $g = 0.0005$  for **(1b)** and 0.0007 for  $(2) \cdot 0.5\text{CH}_2\text{Cl}_2$ ]. Final residual indices were  $R = 0.035$  ( $R' = 0.036$ ),  $S = 1.29$  for **(1b)** and  $R = 0.039$  ( $R' = 0.042$ ),  $S = 1.32$  for  $(2) \cdot 0.5\text{CH}_2\text{Cl}_2$ . \* Analysis of variance showed the weighting schemes to be satisfactory. Final difference electron-density syntheses showed no features of magnitude  $> 0.6$  and  $> 0.36 \text{ e } \text{ \AA}^{-3}$  for **(1b)** and  $(2) \cdot 0.5\text{CH}_2\text{Cl}_2$  respectively. Tables 6 and 7 list the final atomic co-ordinates for the non-hydrogen atoms of **(1b)** and  $(2) \cdot 0.5\text{CH}_2\text{Cl}_2$ . All calculations were carried out with programs of the SHELXTL<sup>17</sup> program package on a Data General Eclipse computer.

*Extended Hückel Molecular Orbital Calculations.*—Hückel parameters<sup>18</sup> for all calculations<sup>19</sup> were taken from ref. 18,

\*  $R = \sum |F_o| - |F_c| / \sum |F_o|$ ;  $R' = \sum w^{\frac{1}{2}} |F_o| - |F_c| / \sum w^{\frac{1}{2}} |F_o|$ ;  $S = [\sum w - (|F_o| - |F_c|)^2 / (\text{N.O.} - \text{N.V.})]^{\frac{1}{2}}$ .

with phosphorus atoms assigned only 3s and 3p valence orbitals. The geometry of the model molecule [ $\text{Mn}(\text{CO})-(\text{H}_2\text{PCH}_2\text{CH}_2\text{PH}_2)(\eta^5\text{-C}_6\text{H}_7)$ ] was taken from the crystal structure of **(1b)** with all C-H distances set to 1.09 Å and P-H lengths 1.44 Å and with hydrogen atoms replacing phenyl substituents. The interaction diagram of Figure 3 was derived from calculations on the component fragments of the model molecule.

### Acknowledgements

We thank the S.E.R.C. for a Research Studentship (to J. B. S.) and the National Science Foundation for financial support (to D. A. S.).

### References

- 1 Part 20, N. G. Connelly, A. R. Lucy, R. M. Mills, J. B. Sheridan, and P. Woodward, *J. Chem. Soc., Dalton Trans.*, 1985, 699.
- 2 R. K. Brown, J. M. Williams, A. J. Schultz, G. D. Stucky, S. D. Ittel, and R. L. Harlow, *J. Am. Chem. Soc.*, 1980, **102**, 981.
- 3 M. Brookhart and M. L. H. Green, *J. Organomet. Chem.*, 1983, **250**, 395.
- 4 R. L. Harlow, R. J. McKinney, and S. D. Ittel, *J. Am. Chem. Soc.*, 1979, **101**, 7496.
- 5 M. R. Thompson, V. W. Day, K. D. Tau, and E. L. Muetterties, *Inorg. Chem.*, 1981, **20**, 1237.
- 6 Y. K. Chung, P. G. Williard, and D. A. Sweigart, *Organometallics*, 1982, **1**, 1053.
- 7 J. C. Calabrese, personal communication, 1984.
- 8 N. G. Connelly and M. D. Kitchen, *J. Chem. Soc., Dalton Trans.*, 1977, 931.
- 9 T. A. Albright, P. Hofmann, and R. Hoffmann, *J. Am. Chem. Soc.*, 1977, **99**, 7546.
- 10 M. R. Churchill and F. R. Scholer, *Inorg. Chem.*, 1969, **8**, 1950.
- 11 R. Hoffmann, *J. Chem. Phys.*, 1963, **39**, 1397; R. Hoffmann and W. N. Lipscomb, *ibid.*, 1962, **36**, 3179, 3489; **37**, 2872.
- 12 R. L. Harlow, R. J. McKinney, and J. F. Whitney, *Organometallics*, 1983, **2**, 1839.
- 13 C. Barbeau and R. J. Dubey, *Can. J. Chem.*, 1974, **52**, 1140.
- 14 C. G. Howard, S. G. Girolami, G. Wilkinson, M. Thornton-Pett, and M. B. Hursthouse, *J. Chem. Soc., Dalton Trans.*, 1983, 2631.
- 15 J. C. Smart and B. L. Pinsky, *J. Am. Chem. Soc.*, 1980, **102**, 1009.
- 16 N. G. Connelly, M. J. Freeman, I. Manners, and A. G. Orpen, *J. Chem. Soc., Dalton Trans.*, 1984, 2703.
- 17 G. M. Sheldrick, SHELXTL programs for use with the Nicolet X-ray system, Cambridge, 1976; updated Göttingen, 1981.
- 18 D. L. Thorn and R. Hoffmann, *Inorg. Chem.*, 1978, **17**, 126 and refs. therein.
- 19 Program ICON 8, J. Howell, A. Rossi, D. Wallace, K. Havabe, and R. Hoffmann, Quantum Chemistry Program Exchange, 1977, **10**, 344.

Received 10th August 1984; Paper 4/1416